ELSEVIER

Chemical Physics 218 (1997) 57–69

Chemical Physics

Simulation of the SiH ($A^2\Delta \rightarrow X\,^2\Pi$) emission spectrum in a silane glow discharge and derivation of an improved set of molecular constants

S. Stamou, D. Mataras, D. Rapakoulias

Laboratory of Plasma Chemistry, Department of Chemical Engineering, University of Patras, P.O. Box 1407, 26500, Patras, Greece

Received 25 November 1996

Abstract

An improved simulation of the rotational intensity distribution of the 0–0 emission band of the $A^2\Delta$–$X\,^2\Pi$ transition of SiH, that is experimentally obtained by optical emission spectroscopy from a silane rf glow-discharge, is reported. The improvements consist in the use of a new term value formula, a recent set of molecular constants and an extended least squares fitting analysis for the micro-optimization of the set of constants. Thus, the rotational temperature of SiH is determined by utilizing a sufficient spectral resolution together with an experimentally determined instrument function of the optical system. The optimum fit of the emission spectrum is obtained for a rotational temperature $T_{ROT} = 2840 \pm 50$ K which is significantly higher compared to those previously reported. Furthermore, an abnormal behaviour of the observed splittings compared to the theoretical calculations is observed, while in two cases experimental measurements of Λ-doublets were performed.

1. Introduction

Electronically excited SiH is the main emitting fragment, resulting from electron collisional dissociative excitation [1], in silane containing rf discharges which are commonly used for thin film microelectronics. Furthermore, these diatomic hydrides are of considerable interest in spectroscopy and astrophysics. The occurrence of SiH in the stellar atmosphere [2,3] combined with its resemblance to the CH radical, make SiH an interesting object for experimental and theoretical studies.

The electronic structure of SiH has been the subject of several experimental [4–11] and theoretical investigations [12–15] concerning mainly the $A^2\Delta$–$X\,^2\Pi$ transition, which is analogous to the 4135 Å band of CH. However, precise information concerning all the energy levels of the SiH radical is not available. For instance, very few attempts to detect SiH by laser magnetic resonance (LMR) have been reported [16,17], in contrast to the CH radical which has been extensively studied by LMR spectroscopy [18–20]. Thus, compared to CH, there are still aspects of the electronic structure of SiH that need to be clarified.

The intensity distribution in the rotational fine structure of electronic transitions, such as $A^2\Delta$–$X\,^2\Pi$, is often used for the measurement of the rotational temperature of the emitting species in various plasma sources [21]. Generally, the measurement

PII S0301-0104(97)00052-9

of these temperatures in non-equilibrium plasmas, can give access to information concerning the electron impact excitation or dissociative excitation processes as a function of the various interrelated plasma parameters and/or its evolution as a function of the discharge space [22].

Among the methods employed for measuring rotational temperature the most widely used is that of the Boltzman plot. However, in the case of SiH, due to the existence of closely placed Λ-doublets, the emission is usually insufficiently resolved, thus not permitting the use of semilogarithmic plot of the line intensities. The method can be applied if the FWHM of the optical system is known, but the accuracy of the resulting rotational temperature measurements is limited [23]. Thus, a simulation of the spectrum is necessary.

The Boltzman plot method is also used to verify whether the distribution of the population on the rotational levels of the excited species is in equilibrium as described by Boltzman statistics [21]. Indeed, the assumption of partial equilibrium of the rotational level population distribution in the $A^2\Delta$ excited state of SiH, has been shown to be valid under the range of conditions used in this work [23]. This is also reenforced by the experimental evidence of collision-induced transfer of the rotational quanta within the $A^2\Delta$, which indicates that a sufficient thermalization of the population of the upper state can be achieved [24]. Boltzman statistics have been similarly found to be valid in the case of SiH^+ which is also formed through dissociative excitation [25], as well as in the case of other species produced by direct electron impact excitation from the ground state [26].

The first attempt to simulate the emission spectrum of SiH in hydrogen diluted silane discharges, has revealed a high rovibrational excitation, i.e. a rotational temperature of 1800 K and a vibrational temperature of 3800 K [27], while the method has been used as is in later works, employing medium to low resolution spectra [28–30]. However, an attempt to use this method for simulating the higher resolution spectra used in the present work, has proven that it is inadequate.

Thus, an extensive testing of the various data and formulas found in literature, towards the minimization of the differences between the experimental and the simulated spectra, is attempted. It is shown that the various formulas and constants used in the simulation program should be dealt with very carefully. More specifically, a new term value formula which takes into account the effect of centrifugal distortion on the spin multiplets is adopted [31]. Furthermore, a more recent set of molecular constants [10] is further micro-optimized applying extended least squares fitting analysis. The optimization procedure is based on a sufficient spectral resolution and an experimentally determined instrument function of the optical system that improves the reliability of the method. Thus, an overall enhancement of the accuracy of the determination of the rotational temperature is achieved. Moreover, the problems related to the prediction of Λ-doubling, which has an important impact for large J, are discussed. In addition, these experiments permit also the experimental measurement of Λ-doubling in two cases, and the identification of preferential Λ-doubling populations.

2. Experimental

The experimental setup is described in detail elsewhere [32]. Briefly, the cell is a 160 mm wide, stainless steel parallel plate discharge chamber with 55 mm in diameter electrodes. Pressure is measured by a capacitance manometer and can be adjusted independently from the flow rate, within the region of interest, by using mass flow controllers and downstream pressure control by a throttling valve. Matheson ultra-high purity silane was used in all cases, while the system was baked out and pumped down to 10^{-7} Torr prior to the experiments. All the measurements are performed in low-pressure and low-power conditions. More specifically, pressure is varied within 40–100 mTorr range, while the peak-to-peak rf voltage is varied from 75 to 200 V. In these conditions, the actual power consumed by the discharge ranges from 0.04 to 0.5 W approximately, as measured with the technique described in [33]. Furthermore, possible formation of powder during the measurements, by homogeneous nucleation in the gas phase, is controlled by using a laser light scattering technique. More specifically, the beam of a HeNe laser is shaped into a light sheet and directed into the interelectrode region of the reactor. In the

existence of particles, the laser light scattered at right angles to the propagating beam, is focused with a lens system in a monochromator set at the specific wavelength of the HeNe laser and the signal from the photomultiplier indicates the presence of particulates. In all the measurements presented here are no powder formation is observed.

The emission from a pure silane discharge is collected by a collimating lens and then focused with a second lens at the entrance slit of a Jobin Yvon THR-1000 1 m focal length monochromator, equipped with a plane ruled grating of 3600 grooves per millimetre. The widths of the entrance and exit slits were 150 μm and 160 μm respectively. The light intensity at the exit slit is recorded using a Hamamatsu 1P28 side-on photomultiplier tube (PMT) with an optimum signal to noise ratio for a cathode voltage of −800 V. The scan speed of the monochromator was 1 Å/min. The FWHM of the instrument is determined using the 4198 Å emission line from an Ar discharge. The shape of the instrument line profile is either triangular or trapezoidal, for equal or unequal slit widths, respectively. However, the difference between the two cases on the peak height is practically negligible permitting the use of a triangular distribution. The experimentally measured FWHM for these slit widths is 0.14 Å. On the other hand, the best resolution for this instrument, i.e. 0,09 Å, was obtained using 110 μm and 120 μm widths of the entrance and exit slits, respectively.

3. Results and discussion

3.1. Experimental and simulation spectra

Fig. 1 presents an experimental spectrum of the 0–0 band of the $A^2\Delta \rightarrow X^2\Pi$ transition of SiH recorded from a 100 mTorr, 0.15 W, radio-frequency (rf) pure silane discharge. A preliminary analysis reveals a partial overlapping of the 0–0 and the 1–1 bands in the region of P_1, P_2 branches of the 0–0 band, whereas the H_δ line (4101.7 Å), possibly observed in silane discharges, is not present, due to the fact that the mean electron energy is far below the 20 eV threshold of H_δ [34], the emission cross section being approximately twenty times smaller than SiH [29]. The equivalent simulated spectrum, using a rotational temperature of 2840 K, as obtained by the method that will be described in the following, is presented in Fig. 2. In this figure are also indicated the line strengths of the six main and the

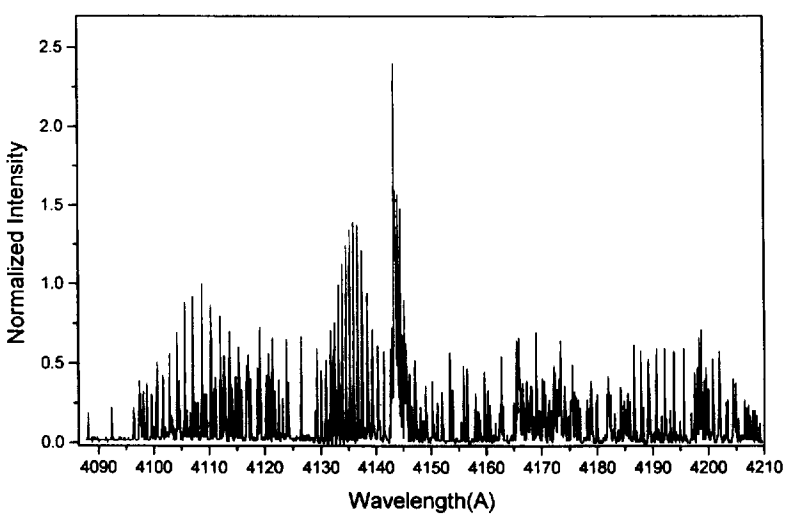

Fig. 1. Experimental emission spectrum of $A^2\Delta$–$X^2\Pi$ transition of SiH recorded from a 100 mTorr pure silane rf discharge. The peak heights have been normalized to the highest peak of R_1 branch, namely $R_1(10.5)$.

six satellite branches emerging from the doublet transition. Furthermore, as Λ-type doubling occurs in the ground state, each lower level is split into e and f sublevels so that each observed peak is composed by two closely placed lines [7], as can be observed in some cases in both the presented experimental and the simulated spectra. Some of the lines missing from the simulated spectrum, as compared to the experimental one, come from the 1–1 band. The Hönl–London formulas given by Kovacs [8] cannot be applied in the cases of the $P_2(2.5)$, $Q_2(1.5)$, $Q_{P21}(2.5)$, $R_{Q21}(1.5)$, $S_{R21}(0.5)$ and $P_{Q12}(1.5)$ lines, however, these factors can be calculated using the method proposed by Hougen [9]. In this work, the Hönl–London factors for the lines mentioned above are calculated by making a series expansion of the Kovacs expressions as a function of $f = J - (\Lambda + 1/2)$ and taking the limit for $f \rightarrow 0$. Furthermore, a detailed peak assignment shows that none of the branches exhibits a peak corresponding to $J > 19.5$.

A more detailed view of the structure of the Q_1 and Q_2 branches using the best possible resolution of the optical system (i.e. 0.09 Å FWHM), that has been recorded in operating conditions of 200 mTorr and 0.25 W, is shown in Fig. 3. Two important features of the spectrum are observable in this figure. The first is the partial overlapping of the $Q_1(10.5)$ and $R_2(2.5)$ lines observed at 4135.33 Å. In lower resolutions this overlapping results in an increase of the specific peak height. This peak has been used systematically in previous works for the calculation of the rotational temperature [28–30]. However, a slight miscalculation of the line positions using a certain set of constants can produce an important change in the peak height resulting in a different rotational temperature. Moreover, if the FWHM of the optical system is used as a parameter in the fitting procedure the uncertainty of the peak height further increases. The specific peak as well as other overlapped peaks are not used in the present work

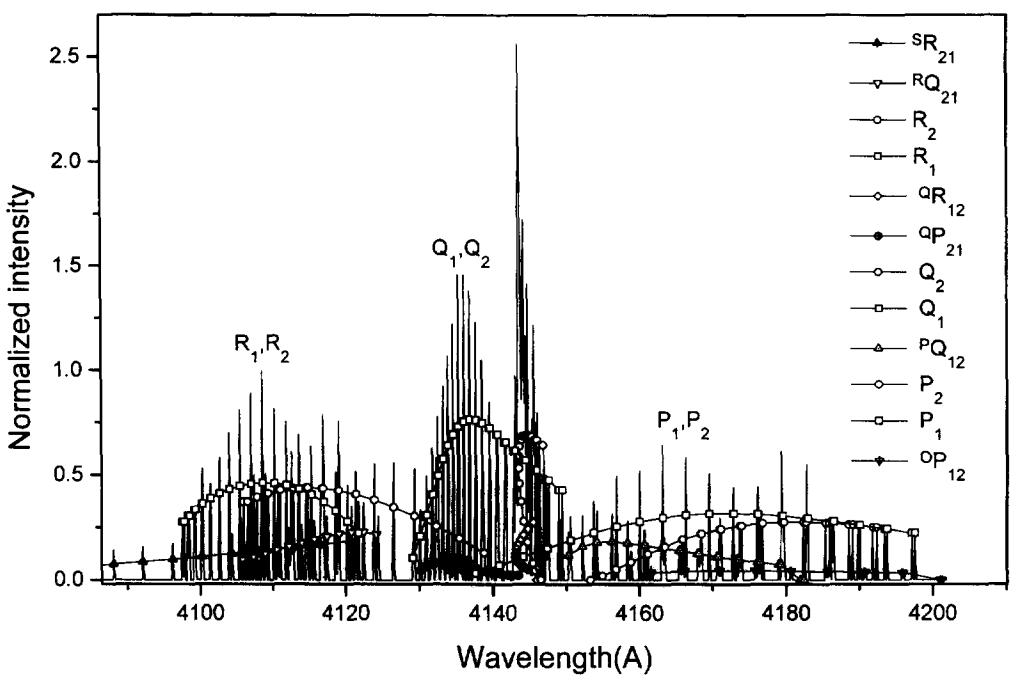

Fig. 2. Simulated spectrum obtained using a rotational temperature of 2840 K. The different symbols indicate line strengths of the six main and the six satellite branches.

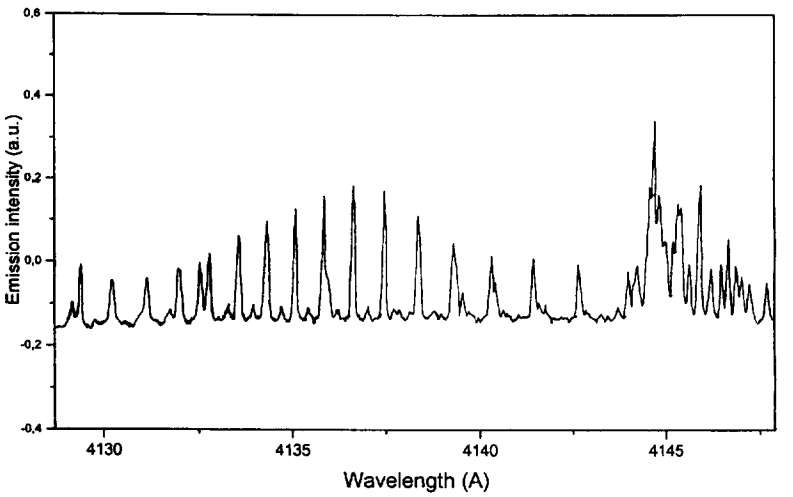

Fig. 3. Experimental spectrum obtained at 200 mTorr with the best possible resolution of the optical system, i.e. 0.09 Å FWHM, presenting Q_1 and Q_2 branches.

for the calculation of the rotational temperature. The second is that the Λ-doublets of the Q1 branch beyond 4140 Å are not split, even in this resolution, indicating abnormal Λ-splitting behaviour. This phenomenon is later discussed in detail.

However, using the resolution of 0.09 Å, small signals are recorded in some cases and thus the applicability of the method is limited in a certain range of conditions that provide a sufficient signal. The results reported here are based on the 0.14 Å FWHM resolution, that has finally adopted and has proven to be sufficient for an accurate determination of the rotational temperature.

3.2. Simulation procedure

3.2.1. Method

A brief review of the procedure used for the simulation of the spectrum, described in detail in literature [35,36], is given here, comprising the following steps:

(1) Calculation of the energy level positions of rotational levels for the $A^2\Delta$ and the $X^2\Pi$ state.

(2) Calculation of the transition wavelengths using the appropriate selection rules.

(3) Calculation of the line strengths using the Hönl–London factors [35] and the Boltzman exponential to account for the population distribution, using T_{ROT} as a parameter.

(4) Convolution of the theoretical spectrum using the known apparatus profile of triangular form.

The improvements presented in this work concern the first and the last steps of the method. Concerning the first step, Klynning et al. [7] have found that for the doublet states neither the well known Hill–van Vleck formula nor the Almy–Horsfall formula can adequately represent the experimentally determined term values. More recently Balasubramanian et al. [31] rederived rigorous expressions for the rotational term values of a diatomic molecule in a doublet electronic state, taking into account the effect of centrifugal distortion on the spin multiplets. The set of equations in this case, excluding terms involving Λ-type doubling, is:

$$T_{1,2} = T - \frac{\gamma}{2}\left(\frac{A_D}{2} + D\right)\Lambda^2 + (B - D) \times X - DX^2 \mp f(J), \quad (1)$$

where $X = (J + 0.5)^2 - \Lambda^2$ and

$$f(J) = \left[\Lambda^2\left\{\frac{(A - 2B)}{2} + \frac{(A_D + 4D)X}{2}\right\}^2 + \left(B - \frac{\gamma}{2} - 2DX\right)^2 X\right]^{1/2}. \quad (2)$$

Furthermore, concerning the last step of the method, the use of an experimentally determined

resolution is one of the advantages of the technique proposed here because in this case T_{ROT} is the only parameter to be determined, avoiding possible erroneous conclusions when FWHM is also an unknown parameter in the least squares fitting procedure. In addition, it permits the indirect evaluation of the consistency of the Λ-doubling formulas and of the molecular constants by comparing experimental and simulation heights of peaks, in cases where close Λ-doublets are not split. Direct evaluation is also possible in cases where the Λ-doublets are clearly resolved.

3.2.2. Molecular constants

The term value formulas mentioned above are used in combination with certain molecular constants, which can be found in the literature in many different sets [5–7,10,16–18]. The use of different sets can give significantly different term values. Moreover, as proposed by Zare et al. [37], sometimes, depending on the forms of the energy level expressions used, the reported molecular constant values fit the experimental line positions, but are not the most appropriate for calculating intensity factors, and in addition, there are problems of purely statistical nature related to the fitting of the observed line positions to the theoretical energy level expressions. Consequently the values of molecular constants must be tested thoroughly to prove their adequacy. The results presented here are obtained using the set of constants provided by Klynning et al. [10], excluding the p and q constants for the calculation of Λ-doubling. The criterion for the use of this particular set is the achievement of the best possible simulation of the observed peak heights and is later discussed in detail.

3.2.3. Λ-type doubling

In the conventional theory of Λ-doubling in $^2\Pi$ states due to van Vleck [38] and Dousmanis et al. [39], the Λ-splitting may be expressed to second order in terms of the parameters p and q, as described in the well-known formula of Mulliken–Christy [40].

$$\Delta F_{1,2} = \left(\tfrac{1}{2}p + q\right)\left[1 \pm \frac{(2-Y)}{X}\right]\left(J+\tfrac{1}{2}\right) \mp \left(\frac{2q}{X}\right) \times \left(J+\tfrac{3}{2}\right)\left(J+\tfrac{1}{2}\right)\left(J-\tfrac{1}{2}\right). \quad (3)$$

The upper signs refer to T_2 sublevels while the lower to T_1, and $X = Y(Y-4) + 4(J+0.5)^2$. However, the observed Λ-doubling for high rotational quantum numbers shows marked deviations from the Mulliken and Christy formula. Hence, corrections which are expressed in terms of the adjustable parameters p_j and q_j are introduced through the phenomenological replacements $p \rightarrow p + p_j J(J+1)$ and $q \rightarrow q + q_j J(J+1)$, to account for the centrifugal distortion effect [41]. Occasionally higher order corrections are required, as for the case of the $X\,^2\Pi$ ground state of CH radical, where Brazier and Brown have used six parameters to fit the experimental Λ-doubling frequencies [42]. However, such kind of data are not available for SiH. Within the many different values for p and q that have been reported in previous works [10,16,17,43,44], those of Brown and Robinson are used [17]. The choice of the particular p and q values is later discussed.

3.2.4. Least squares fitting

The determination of the rotational temperature is based on the minimisation of the difference between the simulated an the experimental spectra. For the actual fitting procedure, twenty-two peaks in total are selected, i.e. eleven peaks corresponding to the same J from each of the Q_1 and R_1 branches. The peaks chosen are not overlapped by any other peak, thus avoiding erroneous calculations when peak heights can change due to a variation of the adjacent or overlapping line positions, and not because of a change of the rotational temperature. T_{ROT} is varied with a step of 20 K to minimise the following error function [29]:

$$\varepsilon = \sum_{i=1}^{22} \left(\frac{I_{i,\mathrm{exp}}}{I_{i,\mathrm{exp}}^{\mathrm{max}}} - \frac{I_{i,\mathrm{sim}}}{I_{i,\mathrm{sim}}^{\mathrm{max}}} \right)^2, \quad (4)$$

where the suffixes 'exp' and 'sim' stand for experimental and simulated intensities respectively, while 'max' stands for maximum intensity. The minimisation of ε is the criterion revealing, not only the effectiveness of the simulation method in general, but also the influence of various 'parameters', such as the values of the molecular constants, on the calculation of the rotational temperature. The basic aim is to obtain the best simulation of the experimental intensity distribution, since the value of the rota-

tional temperature, depends on the distribution of the exact peak heights. Furthermore, the accuracy of the resulting rotational temperature depends drastically on the calculation of the rotational energy levels of the $A^2\Delta$ and this can be evaluated through the least squares fitting procedure.

In conclusion, improvements are made, in the direction of the best fitted intensity distribution, towards a more accurate determination of the rotational temperature. This is achieved by testing all the possible information found in literature, concerning molecular constants and formulas as it will be described in the following paragraphs.

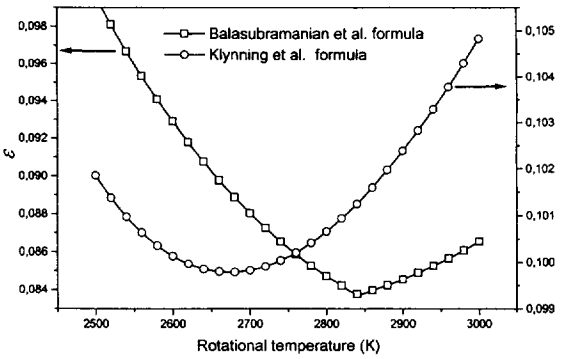

Fig. 4. Error function ε versus rotationaltemperature using different term value formulas.

3.3. Evaluation of term value formulas

Following the reasoning mentioned above, namely, the improvement of the simulation through the least squares fitting procedure, the reliability and adequacy of the term value formulas found in literature is tested.

The first conclusion drawn by comparing the simulation and the experimental spectra, using the Klynning et al. term value formula prior to any subsequent corrections, is related to the observed trend of progressive deviation of the line positions calculated by the simulation for large J quantum numbers [10]. Moreover, the experimental wavenumbers found in their work do not extend for more than $J = 13.5$ specifically for the Q_1 and R_1 branches used here for the calculation of rotational temperature. It is obvious that the lack of data for large J quantum numbers critically affect the values of the calculated molecular constants and thus, any subsequent calculation based on these constants.

The observed discrepancy is partially overcome by using the formula of Balasubramanian et al., taking into account the effect of centrifugal distortion which is an important factor, considering the fact that SiH is expected to have large rovibrational excitation [27], although direct comparison between experimental and calculated wavenumbers is not possible for $J > 13.5$, as mentioned earlier. In Fig. 4 are presented the results of the least squares fitting procedure, resulting in $\varepsilon = 0.08377$ and $T_{ROT} = 2840$ K using the Balasubramanian et al. energy formula, instead of 0.09978 and 2680 K when using the Klynning et al. formula. Note that both these values are obtained using the optimised set of constants as described in Section 3.4. Similar results for ε are given by Tsurubuchi et al., using six peaks, and are in the order of 10^{-3} [29]. This difference in the order of magnitude is comparable to the results presented here and is due to the different number of peaks used in the least squares fitting. Thus, if one selects only six peaks from the twenty-two used in this work the new value for ε is of the same order. This means that an improvement of the accuracy has been achieved, since slight differences in the peak heights between experimental and simulated spectra observable with the resolution used in this work have a significant effect in the value of ε, while for low resolution experiments these slight differences are not observable and thus do not affect the value of ε.

3.4. Evaluation of molecular constants

Systematic testing of molecular constants used in the various formulas of the simulation program has shown that they do not affect the value of rotational temperature in the same extent. Thus, the calculations are mainly affected by the constants concerning the $A^2\Delta$ state, as mentioned before. Furthermore, the A_Π and B_Π molecular constants of the $X^2\Pi$ state have a complex relationship with the calculated peak heights since they are also introduced in the calculation of Hönl–London factors.

The values of the constants tested, are varied within the limits of the standard deviation of the referred values. The optimum values of ε presented bellow are obtained after all the proposed corrections

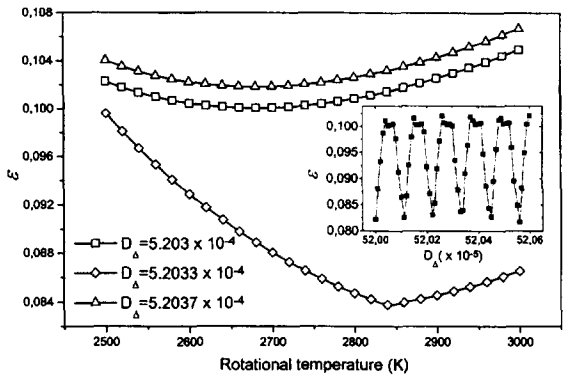

Fig. 5. Least squares fitting results presenting the minimisation of the error function for slightly different values of D_Δ. In the inset is plotted the variation of ε as a function of D_Δ.

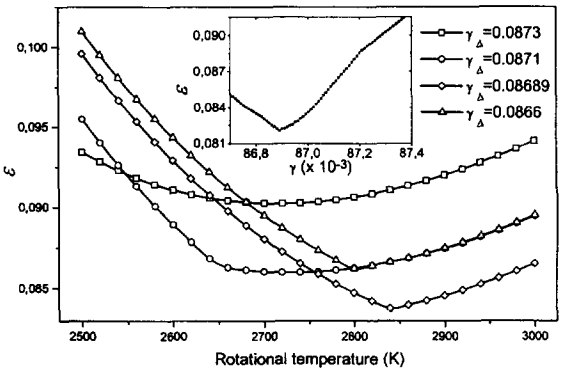

Fig. 6. Least squares fitting results presenting the effect of spin–orbit coupling constant on the rotational temperature. In the inset ε is presented as function of γ_Δ.

are finally adopted, resulting in a $T_{ROT} = 2840$ K. Thus, Fig. 5 presents the effect of the molecular constant $D_\Delta = 5.203 \pm 0.003 \times 10^{-4}$ cm^{-1} on the calculated rotational temperature. For each value of D_Δ, within the limits of standard deviation, ε is minimised at a different temperature. Namely, for $D_\Delta = 5.203 \times 10^{-4}$ cm^{-1} ε takes a minimum value of 0.10007 corresponding to a rotational temperature of $T_{ROT} = 2680$ K, while for the optimum $D_\Delta = 5.2033 \times 10^{-4}$ one calculates the $T_{ROT} = 2840$ K and $\varepsilon = 0.083774$. However as one can observe in the inset of Fig. 5, which presents the variation of ε as a function of D_Δ, this minimization has multiple solutions resulting in approximately the same T_{ROT}. In this case the value which is closer to the mean value reported in literature is chosen.

Similar fitting results concerning the effect of the spin–rotation coupling constant $\gamma = 0.0871 \pm 0.0002$ cm^{-1}, are given in Fig. 6. In this case, the best fit is obtained for $\gamma = 0.0869$ cm^{-1}, whereas a rotational temperature of 2700 K is calculated when a value of 0.0871 cm^{-1} is used. Note for comparison, that if the formula of Klynning et al. is used with the mean values of $\gamma = 0.0871$ cm^{-1} and $D_\Delta = 5.203 \times 10^{-4}$ cm^{-1}, the results are $T_{ROT} = 2680$ K and $\varepsilon = 0.09517$.

The effect of the rotational constant $B_\Pi = 7.38972 \pm 0.00002$ cm^{-1} of the $^2\Pi$ state is presented in Fig. 7. In contrast to the previous cases the minimum is achieved exactly for the mean value of the constant. Since, as stated before, the peaks used for the calculation of T_{ROT} are chosen in a way such as to avoid the influence of small variations of the line positions, this constant is affecting T_{ROT} through the calculation of the Hönl–London factors.

The same testing procedure was performed thoroughly for all the other constants used in the simulation program, except for p and q which are later discussed in detail. As in the case of B_Π, the mean values for the majority of the rest of the constants are adequate for the calculation as shown in the tables below. Namely, in Table 1 are listed the constants concerning $X\,^2\Pi$, while in Table 2 the constants for the $A^2\Delta$ state, finally used in this work.

It must be noted here that the same values are optimum for a series of experimental spectra result-

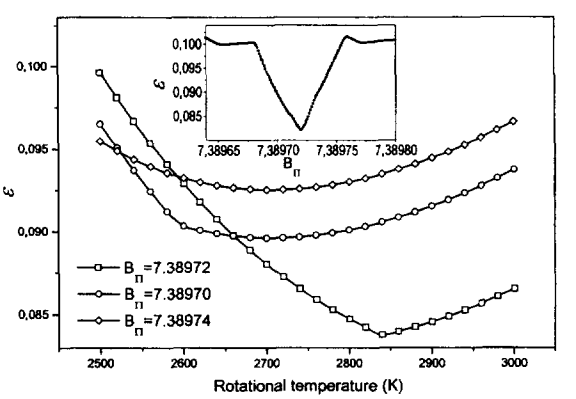

Fig. 7. Calculated rotational temperature for various values of the rotational constant of the ground state B_Π. In the inset ε is presented as function of B_Π.

Table 1
Molecular and Λ-doubling constants of the $^2\Pi$ state used in the simulation

A_Π	B_Π	$D_\Pi \times 10^4$	$A_{D\Pi} \times 10^3$	γ_Π	p_Π	q_Π
142.857	7.38972	3.944	5.09	0	0.083298	0.0083811

ing in different rotational temperatures. These measurements do not yet consist a systematic parametric analysis, which is the purpose of a future study, however, they indicate that the optimised set of constants is representative and does not incorporate erroneous calculations emerging from the discrepancies between simulated and experimental spectra, due to the least squares fitting procedure or possible deviations from Boltzman statistics. The remaining discrepancies, after the optimisation of the set of constants, are caused by other factors, such as the Λ-doubling, which is further discussed, or by predissociation phenomena [11,45]. Thus, a standard deviation of 50 K on the reported value of 2840 K is calculated. Moreover, these results are in agreement with the rationale proposed by Zare et al. [37] as mentioned in Section 3.2.2.

3.5. Λ-type doubling

Λ-type doubling is another very important factor which affects the rotational intensity distribution of not completely resolved spectra, thus having a significant effect on the calculation of rotational temperature. For the calculation of Λ-doubling the constants $p = 0.083298$ and $q = 0.0083811$ given from Brown and Robinson are used [17]. Thus, Fig. 8 presents the results from the least squares fitting procedure comparing the p, q values used in our simulation, with those from Klynning et al., namely $p = 0.08235$ and $q = 0.008305$. In the work of Brown et al. [16] is pointed out that their values, calculated using data from the LMR technique, differ slightly from the values given from Klynning et al., which were calculated using high dispersion plates. Although the last calculation was based on the 'direct approach', it is proven in this work that accurate data, like these provided from the LMR technique, are necessary for the calculation of 'correct' constants, independently of the fitting method used. Thus, even slight variations on the values used are critical when an accurate simulation of the spectrum is to be pursued and therefore no optimisation of p and q is attempted.

Moreover, the Mulliken and Christy formula used here, cannot adequately represent the experimentally observed Λ-doubling. This can be confirmed by comparing carefully the simulation and experimental spectra mainly in three cases, where it can be seen that Λ-doubling is over- or underestimated. First in the R_1 branch which is well resolved up to $J = 19.5$, without being overlapped from any other branch. Second in the part of the Q_1 branch that is not overlapped from the Q_2 branch, for $J = 17.5$ and 18.5. In both cases the Λ-doublets begin to split in the simulation, using the current FWHM, in contrast to the experimental observations (Fig. 3). Finally, the third case in the R_2 branch, presents the most important inconsistency between calculated and experi-

Table 2
Molecular constants of the $^2\Delta$ state used in the simulation

A_Δ	B_Δ	$D_\Delta \times 10^4$	$A_{D\Delta}$	γ_Δ
3.546	7.28280	5.2033	0	0.08689

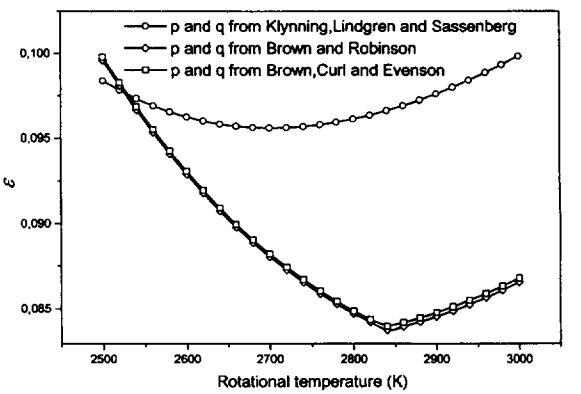

Fig. 8. Least squares fit results presenting the effect of the constants p and q on the calculated rotational temperature.

mental Λ-doubling. In this branch it is possible to measure the experimentally observed splitting, in cases where overlapping does not occur, since Λ-doublets are clearly resolved over $J = 10.5$, and are easily followed up to $J = 15.5$. Thus, Figs. 9 and 10 present calculated Λ-doubling for F_1 and F_2, respectively, while in Fig. 10 are also presented the experimental measurements for $J = 14.5$ and $J = 15.5$, with values 2.50 ± 0.02 cm^{-1} and 3.58 ± 0.02 cm^{-1} respectively. From these figures it appears that F_2 terms exhibit larger Λ-splitting than F_1 terms and thus measurement is possible with the current resolution.

Different curves, which are also presented in these figures, result from possible corrections in the Mulliken and Christy formula in an effort to calculate a different behaviour of Λ-doubling as a function of J, that would include the new experimental values. In addition, this behaviour can be indirectly evaluated for large J, depending on the improvement of the simulated spectrum compared to the experimental one, in regions where branches are overlapped and the overestimation has a more important effect.

The calculated splittings for $J = 14.5$ and $J = 15.5$ using the Mulliken and Christy, i.e. 2.00 cm^{-1} and 2.30 cm^{-1} respectively, are significantly smaller than the experimental values given above. Furthermore, a continuously increasing Λ-doubling with increasing J, is most unfavourable since it has already been remarked that there is overestimation for large J. The introduction of p_j and q_j to account for

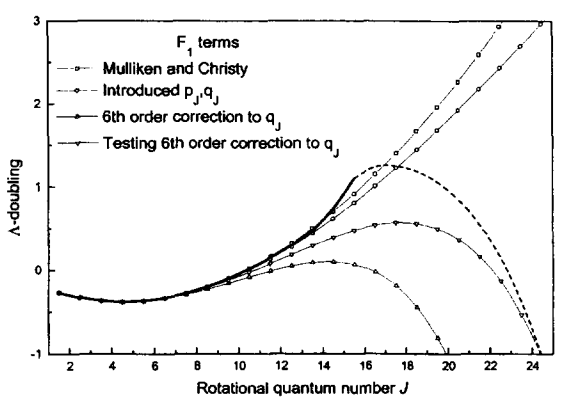

Fig. 9. Calculated Λ-doubling concerning F_1 terms for various formulas. The dashed line presents the desirable evolution of Λ-doubling using an empirical formula.

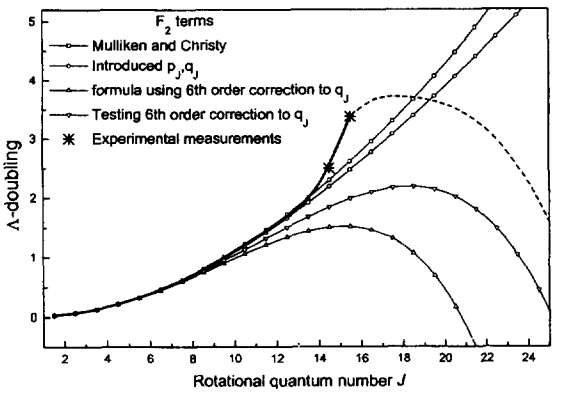

Fig. 10. Calculated Λ-doubling concerning F_2 terms for various formulas. The dashed line presents the desirable evolution of Λ-doubling using an empirical formula that predicts the experimental measurements.

the centrifugal distortion on Λ-doubling appears to have a weak dependence on J, and does not rectify the observed discrepancies, while the experimental values cannot be simulated. The behaviour that has shown the best results in general, and more specifically in the overlapped regions, is similar to the one described by Winkel and Davis for SH [46]. The Λ-doubling components of the $^2\Pi_{3/2}$ multiplet are blended together at low J, move apart to a maximum separation for $J = 16.5$ and merge again at $J = 28.5$ and $J = 29.5$ to cross over and re-separate for still larger J. At the same time the Λ-doubling components of the $^2\Pi_{1/2}$ multiplet are separate at low J, form a single blended line at $J = 10.5$ and $J = 11.5$ while crossing one another, and re-emerge into separated lines for larger J. However, this behaviour was not possible to be reproduced for any pair of p_j and q_j values. Veseth [47] trying to overcome the inconsistency arising when p and q appear not simulating with the same accuracy $^2\Pi_{3/2}$ and $^2\Pi_{1/2}$ levels, has proposed the following empirical formula to express the observed correlation (Obs_{cor}):

$$\mathrm{Obs}_{\mathrm{cor}} = qH(J) + q_J \frac{(J-1/2)(J+1/2)(J+1)(J+3/2)}{X}. \quad (5)$$

In this formula corrections up to the sixth order are incorporated to q_j. The resulting calculations for Λ-doubling using this formula, with $H(J) = 1$ are also presented in Figs. 8 and 9. The behaviour of the curves is quite similar to the one described above. However, in the value of q_j used here, sixth order corrections are not incorporated therefore the desired agreement with experiment is not achieved. Furthermore, variations in the value of q_j were performed to obtain the observed behaviour but were not proved successful. Still, another effort was made to use a higher order empirical formula. However, this formula is not reliable enough, as shown in Figs. 9 and 10 due to the lack of precise data for large J and cannot be used at this point. It must be noted here that no significant change in the rotational temperature measurements is expected, by the estimation of Λ-doubling for large J, since deviations from calculated Λ-doubling have no effect on the twenty-two peaks used in the least squares fit. In cases where optical systems with lower resolution are used to measure rotational temperature from the unresolved spectrum, systematic errors can be obtained due to deviations from the Mulliken and Christy formula.

Finally, unequal Λ-doublet populations were detected. Morespecifically, in the $R_2(10.5)$ peak, which is not overlapped by any near peak, Λ-doublets are clearly but not totally split. Since populations are taken to be proportional to the peak heights, unequal peak heights observed here are a proof of a population imbalance. The same phenomenon is also observed at $R_2(14.5)$ and $R_2(15.5)$ peaks, although less pronounced since these peaks exhibit almost half the intensity of the $R_2(10.5)$ peak and thus it is more difficult to be evaluated. This population imbalance occurs in favour of the e component which appears to be higher than the f component. However, the observed imbalance is rather weak and does not concern $J < 13.5$, as has been reported in Ref. [23]. Thus, the calculation of the rotational temperature is not affected. As it has been explained by Alexander and Dagdigian [48], the imbalance of the Λ-doublet population for high values of N is due to collisional depletion of the $\Pi(A')$ levels ($F_1 e$ or $F_2 f$) and the preferred population of the $\Pi(A'')$ levels ($F_1 f$ or $F_2 e$). Extended investigation of this phenomenon has been reported mainly for the CH radical [49–51], and it appears that a similar situation stands also for the case of SiH. Even though $CH(X\,^2\Pi)$ is a prototypical Hund's case (b) diatomic molecule ($Y = 1.93$) at relatively low values of the total angular momentum J, the rotational wave functions are best described in terms of intermediate coupling between Hund's case (a) and case (b), which is the case of SiH ($Y = 19.35$). Thus the similarity between the $A^2\Pi - ^2\Delta$ systems of CH and SiH radicals also implies a possible similarity in collision-induced transitions [50]. Further theoretical and experimental investigation is not employed here, however a more detailed examination of Λ-doubling in the ground state of SiH is definitely required.

4. Conclusions

The rotational temperature of SiH in silane rf glow-discharge has been determined by optical emission spectroscopy, by simulating the intensity distribution of the rotational fine structure of the 0–0 band of the $A^2\Delta - X\,^2\Pi$ transition.

The main advantages of the method consist in using an improved formula for the calculation of the energy levels [29], together with a recent set of constants [10]. Twenty-two isolated peaks from the R_1 and the Q_1 branches were used in order to avoid interference from overlapping. The intensities of the peaks chosen are well predicted by using the appropriate p and q constants, avoiding the influence of the marked deviation of the calculated Λ-doubling for large J. The experimental determination of the instrument function of the optical system is an important feature of the technique proposed here and it is necessary, when an accurate and reliable measurement is required. Furthermore, the values of the constants used are optimized within the limits of precision of the experimental methods used to obtain them. Thus, D_Δ and γ_Δ were found to have the most significant effect to the minimization function, whereas the use of the mean values for the majority of the other constants was sufficient. The rotational temperature of 2840 ± 50 K obtained from several measurements in pure silane discharges is considerably higher than the 2000 K reported for hydrogen diluted silane [25], however much lower than the 4000 K obtained in a supersonically expanding argon/silane plasma [28]. The method is not fully

applicable in lower resolutions, however it is more reliable, compared to previous simulation attempts and thus is expected to be more accurate even in lower resolutions when a rotational temperature is extracted from the unresolved spectrum. In this last case, if one attempts to minimize the difference between experimental and simulated spectrum, the part of the unresolved spectrum where Λ-doubling is well predicted must be used or else erroneous results are expected.

Moreover, experimental measurements of Λ-doublets were performed in two cases, while abnormal Λ-doubling behavior is observed. In addition, unequal Λ-doublets were also detected in some cases.

The remaining discrepancies between the simulated and experimental spectra, can be due to several factors, such as the already mentioned abnormal Λ-doubling behavior, preferential Λ-doubling and the fact that the existing sets of constants are not calculated using data concerning large J quantum numbers.

Acknowledgements

This work was financially supported by the European Union JOULE project under contract No JOU2-CT94-0403.

References

[1] F.J. Kampas, R.W. Griffith, J. Appl. Phys. 52 (1981) 1285.
[2] H.D. Babcock, Astrophys. J. 102 (1945) 154.
[3] A.J. Sauval, Sol. Phys. 10 (1969) 319.
[4] C.V. Jackson, Proc. R. Soc. (London) 126 (1930) 373.
[5] G.D. Rochester, Z. Phys. 101 (1936) 769.
[6] A.E. Douglas, Can. J. Phys. 35 (1957) 71.
[7] L. Klynning, B. Lindgren, Ark. F. Phys. 33 (1966) 73.
[8] R.D. Verma, Can. J. Phys. 43 (1965) 2136.
[9] W.H. Smith, J. Chem. Phys. 51 (1969) 520.
[10] L. Klynning, B. Lindgren, U. Sassenberg, Phys. Scr. 20 (1979) 617.
[11] G. Herzberg, A. Lagerqvist, B.J. McKenzie, Can. J. Phys. 47 (1969) 1889.
[12] P.C. Jordan, J. Chem. Phys. 44 (1966) 3400.
[13] P.E. Cade, W.M. Huo, J. Chem. Phys. 47 (1967) 649.
[14] B. Wirsam, Chem. Phys. Lett. 10 (1971) 180.
[15] M. Lewrentz, P.J. Bruna, S.D. Peyerimhoff, R.J. Buenker, Mol. Phys. 49 (1983) 1.
[16] J.M. Brown, R.F. Curl, K.M. Evenson, J. Chem. Phys. 81 (1984) 2884.
[17] J.M. Brown, D. Robinson, Mol. Phys. 51 (1984) 883.
[18] K.M. Evenson, H.E. Radford, M.M. Moran Jr., Appl. Phys. Lett. 18 (1971) 426.
[19] J.M. Brown, K.M. Evenson, J. Mol. Spectrosc. 98 (1983) 392.
[20] J.T. Hougen, J.A. Mucha, D.A. Jennings, K.M. Evenson, J. Mol. Spectrosc. 72 (1978) 463.
[21] I. Ishii, A. Montaser, Spectrochim. Acta 46B (1991) 1197.
[22] G. Turban, B. Drevillon, D. Mataras, D.E. Rapakoulias, in: Plasma Deposition of Amorphous Silicon Based Materials, G. Bruno, P. Capezzuto, A. Madan (Eds.), Academic Press, London, 1995, p. 63.
[23] S. Stamou, N. Spiliopoulos, D. Mataras, D. Rapakoulias, J. High Temp. Chem. Proc., to be published.
[24] J.P.M. Schmitt, P. Gressier, M. Krishnan, G. de Rosny, J. Perrin, Chem. Phys. 84 (1984) 281.
[25] J. Perrin, J.F.M. Aarts, Chem. Phys. 80 (1983) 351.
[26] A. Chelouah, E. Marode, G. Hartmann, S. Achat, J. Phys. D: Appl. Phys. 27 (1994) 940.
[27] J. Perrin, E. Delafosse, J. Phys. D: Appl. Phys. 13 (1980) 759.
[28] J. Perrin, J.P.M. Schmitt, Chem. Phys. 67 (1982) 167.
[29] S. Tsurubuchi, K. Motohashi, S. Matsuoka, T. Arikawa, Chem. Phys. 161 (1992) 493.
[30] G.J. Meeusen, E.A. Ershov-Pavlov, R.F.G. Meulenbroeks, M.C.M. van de Sanden, D.C. Schram, J. Appl. Phys. 71 (1992) 4156.
[31] T.K. Balasubramanian, A.S.P. Rao, R. D'Souza, N.A. Narasimham, Acta Phys. Hung. 55 (1984) 27.
[32] D. Mataras, S. Cavadias, D. Rapakoulias, J. Appl. Phys. 66 (1989) 119.
[33] N. Spiliopoulos, D. Mataras, D.E. Rapakoulias, J. Vac. Sci. Technol. A 14 (1996) in press.
[34] Quixin Lin, Xuangying Lin, Yunpeng Yu, Hong Wang, Kiayi Chen, J. Appl. Phys. 74 (1993) 4899.
[35] I. Kovacs, Rotational Structure in the Spectra of Diatomic Molecules, Adam Hilger, London, 1969, p. 115.
[36] G. Herzberg, Molecular Spectra and Molecular Structure, Vol. 1, D. Van Nostrand, New York, 1950, p. 212.
[37] R.N. Zare, A.L. Schmeltekopf, W.J. Harrop, D.L. Albritton, J. Mol. Spectrosc. 46 (1973) 37.
[38] J.H. van Vleck, Phys. Rev. 33 (1929) 467.
[39] G.C. Dousmanis, T.M. Sanders, C.H. Townes, Phys. Rev. 100 (1955) 1735.
[40] R.S. Mulliken, A. Christy, Phys. Rev. 38 (1931) 87.
[41] L. Veseth, J. Phys. B: Atom. Mol. Phys. 3 (1970) 1677.
[42] C.R. Brazier, J.M. Brown, Can. J. Phys. 62 (1984) 1563.
[43] D.L. Cooper, W.G. Richards, J. Chem. Phys. 74 (1981) 96.
[44] R.S. Freedman, A.W. Irwin, Astron. Astrophys. 53 (1976) 447.
[45] T. Carlson, N. Duric, P. Erman, M. Larsson, J. Phys. B: Atom. Mol. Phys. 11 (1978) 3667.
[46] J. Winkel, S.P. Davis, Can. J. Phys. 62 (1984) 1420.

[47] L. Veseth, Mol. Phys. 21 (1971) 287.
[48] M.H. Alexander, P.J. Dagdigian, J. Chem. Phys. 80 (1984) 4325.
[49] M.H. Alexander, P.J. Dagdigian, J. Chem. Phys. 101 (1994) 7468.
[50] S.M. Ball, G. Hancock, M.R. Heal, J. Chem. Soc. Faraday Trans. 90 (1994) 523.
[51] P.J. Dagdidgian, M.H. Alexander, K. Liu, J. Chem. Phys. 91 (1989) 839.